JOURNAL OF GEOPHYSICAL RESEARCH, VOL. 112, A10222, doi:10.1029/2007JA012367, 2007

Ground magnetometer observation of a cross-phase reversal at a steep plasmapause

Z. C. Kale,[1,2] I. R. Mann,[1] C. L. Waters,[3] J. Goldstein,[4] F. W. Menk,[3] and L. G. Ozeke[1]

Received 26 February 2007; revised 25 June 2007; accepted 13 July 2007; published 27 October 2007.

[1] The cross-phase technique employs ground-based magnetometer data in order to determine the resonance frequency of a geomagnetic field line. Typically, a positive cross-phase maximum identifies the field line resonance frequency, but occasionally, a negative cross-phase maximum is observed and is believed to be a feature of the steep density gradient at the plasmapause. For a few hours during the local morning of 14 May 2001 the cross-phase maximum, observed using two pairs of ground-based magnetometer stations from the European sector, with midpoints at L = 3.16 and L = 3.34, reversed polarity from positive to negative. All other British Geological Survey, Sub-Auroral Magnetometer Network, and International Monitor for Auroral Geomagnetic Effects (IMAGE) magnetometer array station pairs examined between L = 2.39 and L = 6.54 showed a positive cross-phase maximum throughout the day. The Imager for Magnetopause-to-Aurora Global Exploration (IMAGE) satellite made an excellent close magnetic conjunction with these ground-based magnetometer arrays on this day, and data from the IMAGE Radio Plasma Imager instrument show a very steep plasmapause in this region during this UT interval. IMAGE Extreme Ultraviolet Imager global plasmasphere images show that the plasmapause moved outward through the day, passing through the region of the observed negative cross-phase maxima. This rare observation of a negative cross-phase maximum occurs at the location of a plasmapause with a gradient steeper than r^{-8} and thus is in agreement with theory. The two cross-phase peak polarity reversals are explained by the evolution of the local density profile.

Citation: Kale, Z. C., I. R. Mann, C. L. Waters, J. Goldstein, F. W. Menk, and L. G. Ozeke (2007), Ground magnetometer observation of a cross-phase reversal at a steep plasmapause, *J. Geophys. Res.*, *112*, A10222, doi:10.1029/2007JA012367.

1. Introduction

[2] The plasmapause is a highly dynamic boundary between the relatively dense plasmasphere and the more rarefied plasma trough regions. The density gradient at the plasmapause can vary azimuthally, and along a particular meridian it may be steep or shallow, depending on the particular time history of that region [e.g., *Carpenter and Anderson*, 1992; *Dent et al.*, 2006].

[3] A steep plasmapause is the cause of, or at least associated with, certain space physics phenomena. *Fraser et al.* [2002] mention that it is the source of certain boundary waves, and *Carpenter* [1978] describes unique whistler mode ground signal observations in the region just beyond a steep plasmapause gradient. A steep plasmapause is the boundary of cavity resonance modes in the plasmasphere [e.g., *Allan et al.*, 1996], or similar virtual cavity resonances [e.g., *Lee and Kim*, 1999; *Waters et al.*, 2002]. On a smaller scale, plasmaspheric notches spanning 3–4 h of local time, causing a low L shell steep plasmapause, have been observed as source regions for kilometric continuum radiation [*Green et al.*, 2004]. Also, stable auroral red (SAR) arc excitation is believed to be a result of ring current ions interacting with plasmaspheric electrons near a steep plasmapause [*Shiokawa et al.*, 2001], possibly via ion cyclotron waves [*Thorne and Horne*, 1992].

[4] Geomagnetic field lines can support shear Alfvén waves in the ULF frequency range and so may be excited at their local resonance frequency (eigenfrequency). The resonance frequency, f_r of a field line is dependent upon the length of the field line, l, the magnetic field strength, B, and the distribution of mass density along it, ρ, $f_r \propto B/l\sqrt{\rho}$. The eigenfrequency is dominated by the equatorial low Alfvén speed region. Therefore, if field line resonance frequencies are monitored, and a geomagnetic field geometry and a form for field-aligned mass density variation are assumed, then the equatorial plasma mass densities may be determined [e.g., *Waters et al.*, 1991a, 1996].

[5] Radial density variations in the equatorial plane may be described by an inverse power law, $r^{-\alpha}$ [e.g., *Carpenter and Smith*, 1964]. *Poulter et al.* [1984] explain that in a

[1]Department of Physics, University of Alberta, Edmonton, Alberta, Canada.
[2]Formerly Z. C. Dent.
[3]School of Mathematical and Physical Sciences and CRC for Satellite Systems, University of Newcastle, Callaghan, New South Wales, Australia.
[4]Space Science and Engineering Division, Southwest Research Institute, San Antonio, Texas, USA.

0148-0227/07/2007JA012367$09.00

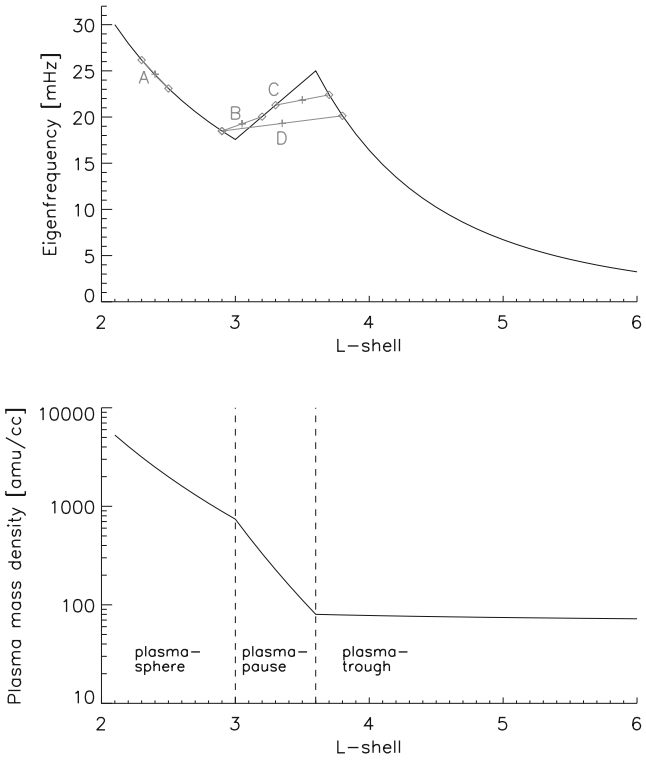

Figure 1. (top) Model eigenfrequency continua showing the expected eigenfrequency variation as a function of L shell. Values shown are similar to those monitored throughout this study. (bottom) Plasma mass density as a function of L shell calculated using the eigenfrequency values in Figure 1 (top) and assuming a dipolar magnetic field geometry and r^{-1} radial density distribution along field lines. See text for details.

dipolar field geometry, the toroidal mode eigenfrequency decreases with increasing L for $\alpha \lesssim 8$; is constant with increasing L for $\alpha = 8$; and increases with increasing L for $\alpha > 8$. Typically, a monotonic decrease of eigenfrequency with increasing L is expected in the plasmasphere and plasma trough, and an increase of eigenfrequency with increasing L occurs across a steep plasmapause [e.g., *Orr and Hanson*, 1981; *Menk et al.*, 2004]. Figure 1 (top) schematically shows the eigenfrequency response with L shell corresponding to the density profile shown in Figure 1 (bottom), which represents the plasmasphere, a steep plasmapause, and the plasma trough regions. Note that in the absence of a sufficiently steep plasmapause density gradient there would be no positive eigenfrequency gradient along this profile. The grey diamonds joined with a line labeled A show the location of notional ground-based magnetometers, and the crosses show the location of the midpoint and the eigenfrequency which will be determined via the cross-phase technique. In this scenario, both magnetometers are at the foot points of field lines which extend to the plasmasphere region. Examples B, C, and D are explained in section 3.

[6] The cross-phase technique examines the amplitude and phase spectra from two latitudinally separated ground-based magnetometers in order to determine the eigenfrequency of a field line with a footprint assumed to be near the latitudinal and longitudinal midpoint between those two magnetometers [e.g., *Waters et al.*, 1991b]. Note that broadband fast mode waves are assumed to drive field line oscillations, and the resonance frequency of a particular field line may not provide the dominant power in the spectrum. Driven Alfvén waves may be treated as forced, damped simple harmonic oscillators [e.g., *Gough and Orr*, 1984]. To illustrate the difference between positive and negative eigenfrequency gradients on the resulting cross-phase (phase difference), amplitude ratio, and amplitude difference, Figure 2 presents some simple calculations of the response of forced, damped simple harmonic oscillators with eigenfrequencies of 20 and 25 mHz. Figure 2 is based on Figure 1 of *Waters et al.* [1991a]. Figures 2a and 2c show the amplitude and phase response, respectively, as a function of frequency for each of the field lines. These show the expected amplitude peak and 180° phase change which is expected through the resonance frequencies. The resonance frequency of the field line with a foot point midway between the foot points of the two field lines being modeled is identified where the amplitude difference of 0, and amplitude ratio of 1 (both with a negative gradient), and the cross-phase shows a local maximum at a value > 0 (i.e., the phase difference maximizes with a positive value). Note that for the positive eigenfrequency profile gradient (Figure 2, right), the amplitude difference and amplitude ratio (Figure 2f) pass through 0 and 1, respectively, with positive gradients, and the cross-phase (Figure 2h) has a local minima at a value < 0 (i.e., a negative valued local maximum of phase difference).

[7] Note that a positive cross-phase maximum, as shown in Figure 2g, is usually referred to as a cross-phase peak; and *Waters* [2000] introduced the expression negative cross-phase maximum to describe the result shown in Figure 2h. For the purpose of this manuscript, the terms "positive cross-phase maximum" and "negative cross-phase maximum" will be used.

[8] A positive cross-phase maximum identifies a region where a negative eigenfrequency gradient exists between the two ground stations (i.e., $\alpha \lesssim 8$), such as is expected in the plasmasphere or plasma trough regions. For a positive eigenfrequency gradient (i.e., $\alpha > 8$), such as across a steep plasmapause, a negative cross-phase maximum is expected. A trend of constant frequency with L shell (i.e., $\alpha = 8$) would cause the cross-phase maxima to be suppressed. Note that if both magnetometers are monitoring field lines with the same eigenfrequency value and with the eigenfrequency continua passing through one or two turning points between those L shell locations (e.g., L = 2.75 and L = 3.30 or L = 2.75 and L = 3.80), then a suppressed cross-phase maximum would also be expected [e.g., *Milling et al.*, 2001].

[9] The potential for constant eigenfrequency with L at the plasmapause was predicted by *Loto'aniu et al.* [1999] and has been observed by *Milling et al.* [2001]. *Waters* [2000] showed an observed negative cross-phase maximum and suggested that it was a feature of the plasmapause. *Denton et al.* [2006] also described observing a negative cross-phase maximum at one L shell along a meridian, and suggested it could indicate the location of the plasmapause.

[10] Cold magnetospheric plasma may be monitored in situ using satellite instruments, or remotely using satellite or

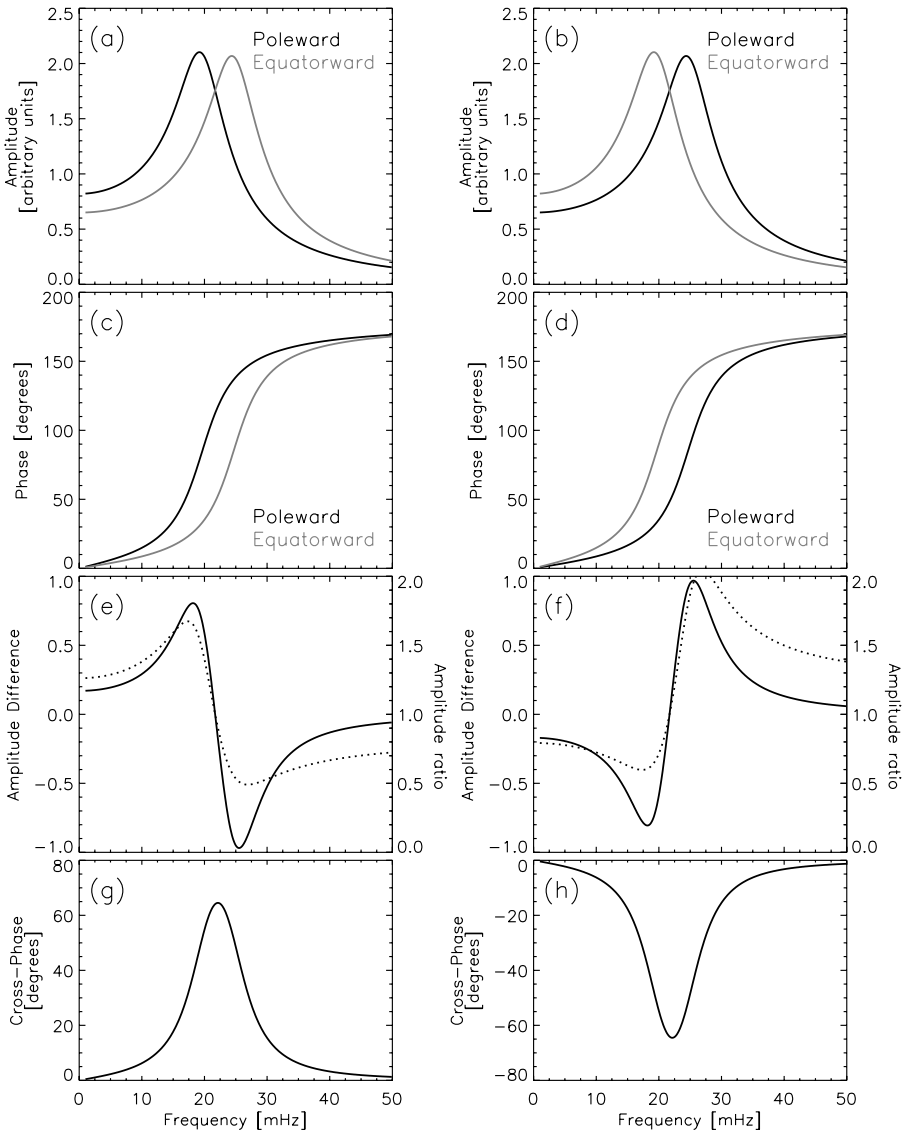

Figure 2. Modeled amplitude and phase response as a function of driving frequency for two field lines with foot points along the same meridian, one poleward and one equatorward. (left) Response for a negative eigenfrequency profile gradient with L shell between the two field lines (i.e., typical plasmasphere or plasma trough region), with f_{pol} = 20 mHz and f_{eq} = 25 mHz. (a) Amplitude; (c) phase; (e) amplitude difference ($A_{pol} - A_{eq}$, solid line) and amplitude ratio (A_{pol}/A_{eq}, dotted line); (g) cross-phase ($\phi_{pol} - \phi_{eq}$). (right) Similar plots, but for a positive eigenfrequency profile gradient (i.e., a steep plasmapause region), with f_{pol} = 25 mHz and f_{eq} = 20 mHz.

ground-based instruments [e.g., *Lemaire et al.*, 1998; *Menk et al.*, 2004]. The present study uses IMAGE satellite Radio Plasma Imager (RPI [e.g., *Reinisch et al.*, 2000; *Goldstein et al.*, 2003]) and Extreme Ultraviolet Imager (EUV [e.g., *Sandel et al.*, 2000]) instruments, and ground-based magnetometers in the European sector to compare the cross-phase response, plasmapause density gradient and plasmapause location through 14 May 2001.

2. Instrumentation and Data Analysis

[11] The cross-phase technique has been employed using a selection of European sector ground-based magnetometers belonging to the Sub-Auroral Magnetometer Network (SAMNET, http://www.dcs.lancs.ac.uk/iono/samnet/ [e.g., *Yeoman et al.*, 1990]), International Monitor for Auroral Geomagnetic Effects (IMAGE) http://www.ava.fmi.fi/image/ [e.g., *Lühr et al.*, 1998]) and British Geological Survey (BGS, data available from SAMNET) arrays. These are shown in Figure 3.

[12] For the present study, where a negative (positive) cross-phase maximum was observed, the standard amplitude and phase responses for a positive (negative) eigenfrequency profile gradient were used to identify the local field line resonance frequency (see Figure 2).

[13] At the three magnetometer stations which showed a negative cross-phase maximum (ESK, L = 2.78; GML, L = 3.08; and LER, L = 3.63), the single-station power ratio

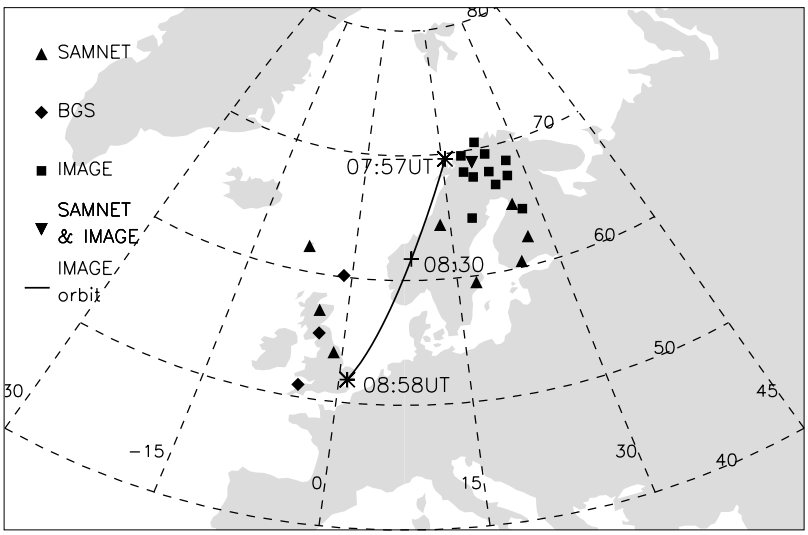

Figure 3. Map showing locations of the ground-based magnetometers employed in this study, and the northern hemisphere ground magnetic footprint of the IMAGE satellite inbound orbit during the intervals when RPI data were used for this study. Geographic coordinate grid lines and the time intervals of the IMAGE RPI data sets are shown. Satellite mapping data were obtained from SSCWeb, http://sscweb.gsfc.nasa.gov, assuming Tsyganenko 89 external and IGRF internal geomagnetic fields.

technique, described by *Baransky et al.* [1990] and *Menk et al.* [2004], was also employed in order to obtain an estimate of the local eigenfrequency.

[14] By assuming a geomagnetic field topology and radial density distribution along the field line, the observed eigenfrequency values may be inverted into equatorial plasma mass density values. For this study both dipolar and Tsyganenko 01 (T01 [*Tsyganenko*, 2002a, 2002b]) geomagnetic field topologies and an r^{-m} radial density distribution along field lines, with m = 1, have been assumed. *Menk et al.* [1999] found the value of m is highly variable, with values between 1 and 6, and that the chosen value is not critical for obtaining reliable estimates of equatorial plasma mass density.

[15] The RPI instrument on board the elliptically orbiting IMAGE satellite passively measured the ambient electric field in order to determine the local plasma frequency, and thus the in situ electron number density [e.g., *Reinisch et al.*, 2000; *Goldstein et al.*, 2003]. For this study, in situ electron number density values, obtained at $37° \geq \text{MLAT} \geq 3°$, have been mapped to the equatorial plane assuming a r^{-1} radial density distribution. This value is consistent with the value of m employed for the cross-phase derived plasma mass density values. Because of the IMAGE satellite orbit, this mapping has greatest effect on the high invariant latitude plasma trough flux tubes. In the vicinity of the plasmapause this mapping resulted in a ~9% decrease in the electron number density value at the equator as compared with the in situ value, but the inferred plasmapause location was unchanged. The maximum error associated with the in situ electron number density values arises due to determining the electron plasma frequency, and this is assumed to be 12% [*Dent et al.*, 2003]. Figure 3 also shows the ground-magnetic foot point of the IMAGE satellite orbit during the time interval for which RPI data are presented. For this study the equatorial electron number density has been converted to a plasma mass density value by assuming a solely H^+ plasma. As the admixture of heavier ions (He^+ and O^+) is unknown, none have been assumed. Note however, that the concentration of heavy ions may not be constant throughout the magnetosphere. *Fraser et al.* [2005] and *Dent et al.* [2006], for example, discuss the presence of an oxygen torus in the vicinity of the plasmapause. This is discussed in the context of this study in section 3.

[16] The EUV Imager on board the IMAGE satellite provided a unique single-instrument view of the global plasmasphere [e.g., *Sandel et al.*, 2000]. It detected 30.4 nm ultraviolet light which had been resonantly scattered by the He^+ population of the plasmasphere. The images produced have spatial and temporal resolutions of ~0.1 R_E and ~10 min, respectively, in two-dimensional line-of-sight integrated pictures [e.g., *Goldstein et al.*, 2003, 2004]. The plasmapause location values presented in this paper have been determined via visual inspection of EUV images which have been mapped to the equatorial plane (as described for a single point by *Goldstein et al.* [2003]). *Goldstein et al.* [2003] note that the uncertainty associated with these values is dependent upon the sharpness of the plasmapause, and is about 0.2 R_E for a sharp He^+ edge, and 0.4–0.8 R_E for diffuse structures.

3. Results and Discussion

[17] The event examined for the study presented in this manuscript took place on 14 May 2001. This day was the first day of recovery after renewed geomagnetic activity occurring during the recovery phase of a moderate geomagnetic storm which occurred on 7 May.

[18] Figure 4 shows the H component (i.e., geomagnetic north-south) dynamic cross-phase spectra for the ESK-LER and GML-LER station pairs (midpoint L = 3.16 and 3.34, respectively) for 14 May 2001. The local eigenfrequency is usually shown by a band of positive maxima in cross-phase through the dayside sector. In Figure 4, a band of positive,

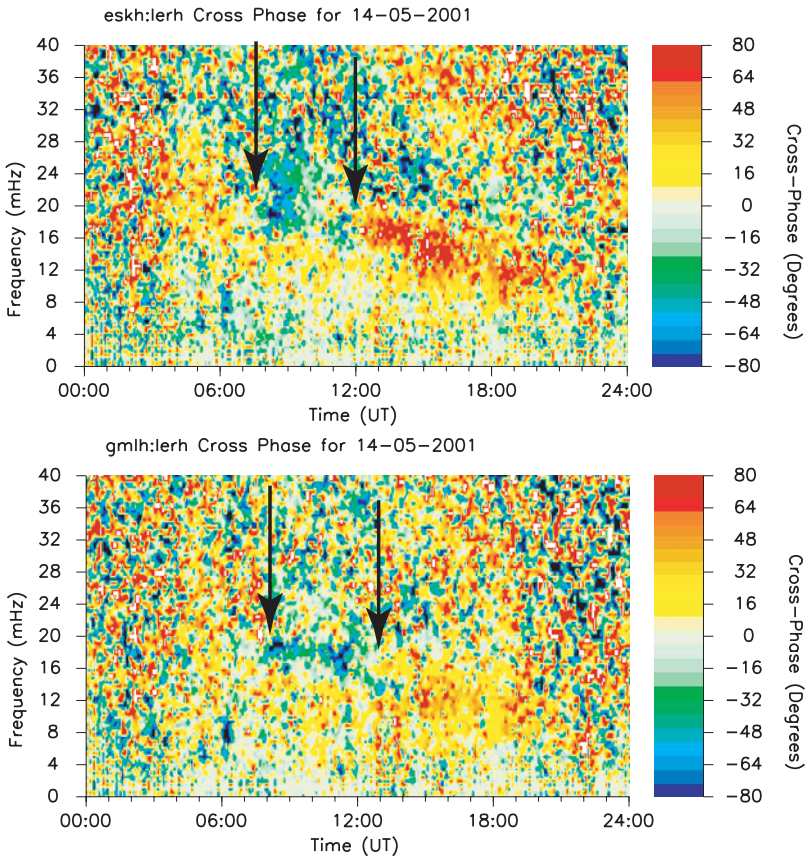

Figure 4. Dynamic cross-phase spectra of the (top) ESK-LER and (bottom) GML-LER station pairs (L = 3.16 and L = 3.34, respectively). The cross-phase maxima are apparent at ~25–100 mHz between ~0400–2000 UT. Polarity reversals of the cross-phase maxima are apparent at approximately 0730 UT and 1200–1230 UT (shown by arrows).

then negative, then positive cross-phase maximum is seen from approximately 10 to 30 mHz between 0400 and 2000 UT. The polarity of the cross-phase maxima reverses at approximately 0730 UT and 1200–1230 UT, as indicated by the black arrows in each plot. Note that these trends are clearer when a low-power cutoff is employed (not shown).

[19] Figure 5 shows eigenfrequency and plasma mass density profiles determined via the cross-phase technique. Note that the dipole model derived densities are plotted versus the ground midpoint L shell, and the T01 model derived densities are plotted versus the ground midpoint magnetic latitude. The four rows represent two intervals during which a negative cross-phase maximum was monitored at L = 3.16 and L = 3.34 (0840 UT and 1100 UT), and two from earlier and later intervals, when only positive cross-phase maxima were monitored across the entire ground-based magnetometer array (0600 UT and 1420 UT). These times each represent the midpoint of a 1-h time interval for which the cross-phase or power ratio technique was employed (using 20–50 min data windows). Note that the results for the single-station power ratio technique (for L = 2.78, 3.08 and 3.63; ESK, GML and LER, respectively) and those determined via positive and negative cross-phase maxima are plotted with different symbols. The grey hashed area highlights the $3.16 \leq L \leq 3.34$ region where the cross-phase maxima polarity reversal was monitored. Error bars associated with the plotted cross-phase derived values represent the uncertainty associated with determining the eigenfrequencies. In Figures 5b, 5e, 5h, and 5k, a density $\propto r^{-8}$ curve is also plotted for comparison.

[20] The eigenfrequencies, determined via the cross-phase technique, show typical monotonically decreasing plasmaspheric and plasma trough trends with L for $L < 3$ and $L > 4$, respectively, and the corresponding density profiles show typical values for these regions. The dipole and T01 derived density profiles show very similar trends, but the T01 derived densities are lower than the dipole derived densities at higher invariant latitudes/L shells, where the T01 model deviation from a dipolar geometry is larger. The dipole derived density profiles for all time intervals show that density decreases with L between $L \sim 3$ and $L \sim 4$, indicating the plasmapause. Note that at all times the plasmapause density gradient with L, between L = 3 and L = 4, is close to the r^{-8} curve, which marks the boundary between a positive or negative eigenfrequency gradient, and thus a negative or positive cross-phase maximum, respectively.

[21] The RPI determined density profile is presented in Figure 5e (circles) and shows a steep density gradient between L = 3.0 and L = 3.2, confirming that the cross-phase maximum polarity reversals occurred in the vicinity of the plasmapause. The differing RPI and cross-phase

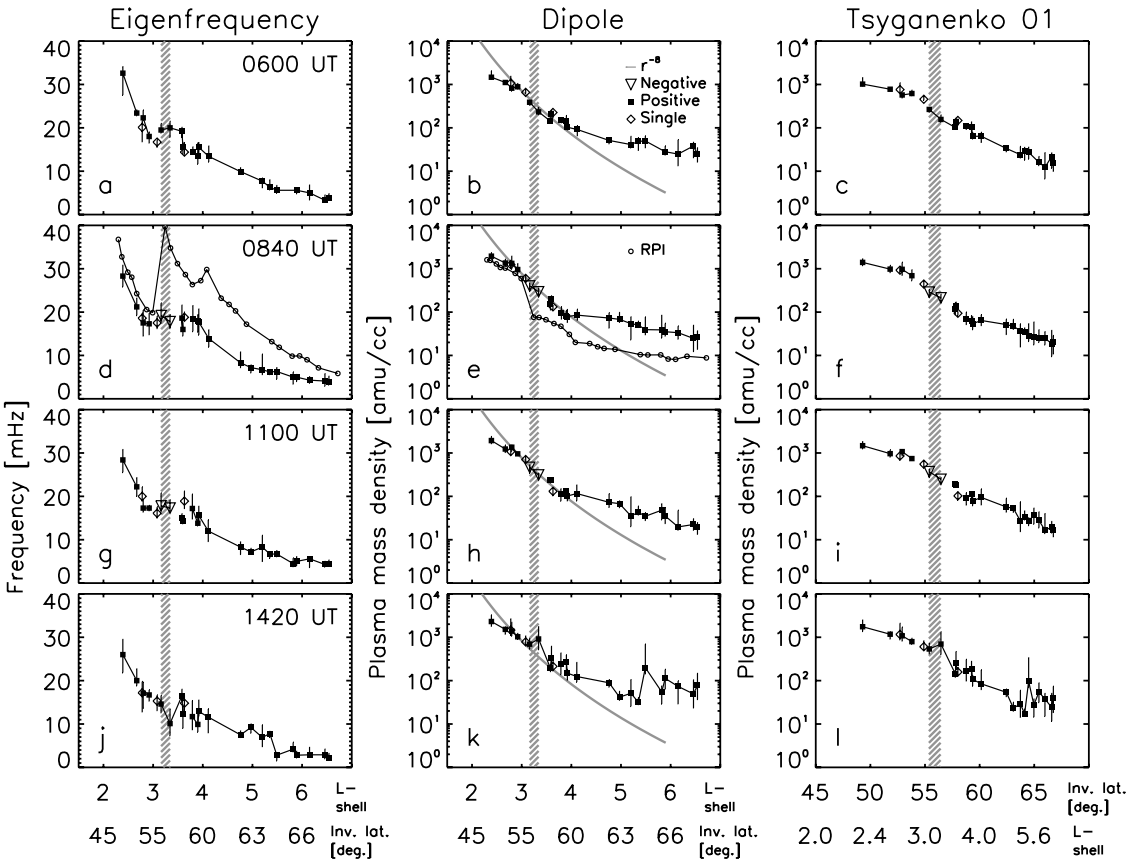

Figure 5. Eigenfrequency and plasma mass density profiles at four intervals on 14 May 2001. Figures 5a, 5b, and 5c (Figures 5d, 5e, and 5f) represent the 0600 UT (1100 UT) interval, etc. Figures 5b, 5c, 5e, 5f, 5h, 5i, 5k, and 5l represent equatorial mass densities determined assuming dipolar and Tsyganenko 01 (T01) magnetic field geometries, respectively. Also plotted are IMAGE RPI derived electron number density and eigenfrequency values (Figures 5d and 5e). Note that lines are drawn connecting data points only to guide the eye. See text for details.

determined densities for L > 4.0 are due to the presence of an enhanced heavy ion population in the form of a torus outside a recently depleted plasmapause [see *Dent et al.*, 2006; *Fraser et al.*, 2005]. Note that the cross-phase determined plasmapause gradient is significantly shallower than that shown by the RPI data. *Menk et al.* [2004] explain that if the ground stations map to either side of the eigenfrequency turning points at the plasmapause, then the assumption of a monotonically varying eigenfrequency profile is invalid. Under such circumstances the derived plasma mass density profile near the plasmapause will be artificially smoothed. This is shown schematically in Figure 1, where examples B, C and D show how a magnetometer station pair which straddles different regimes may result in an incorrect eigenfrequency being determined. For example, in the case of example B, one magnetometer is at the foot point of a field line which maps to the plasmapause region, while the other is at the foot point of a field line mapping to the plasma trough region. Because of the local eigenfrequency minima occurring along the eigenfrequency profile between these two points, the resonance frequency value determined via cross-phase analysis will be overestimated. Consequently, the derived plasma mass density will underestimated.

[22] These effects are also the likely cause of the apparent eigenfrequency increase with time between 0600 UT and 0800 UT, localized to the $3.5 \lesssim L \lesssim 4.0$ region. During the postdawn morning sector, flux tubes in both the plasmasphere and plasma trough are expected to replenish with plasma following nighttime loss of plasma to the ionosphere. This will act to decrease field line eigenfrequencies as a function of time. A localized decrease of density is shown along both the dipole and T01 derived density profiles. At the same time, the T01 model predicted shortening of all of the field lines modeled. (This could be the result of the slight decrease of geomagnetic activity, and/or the rotation of the field lines out of the dawn flank, where field line stretching occurs). Field line shortening would act to increase the eigenfrequency. A scenario of field line shortening and plasma density increase at all field lines does not explain the localized eigenfrequency increase with time at such a low L shell in the morning sector. Instead, if the ground magnetometer station pairs monitoring $3.5 \lesssim L \lesssim 4.0$ were at the foot points of field lines mapping to two different plasma regions, then an incorrectly high or low

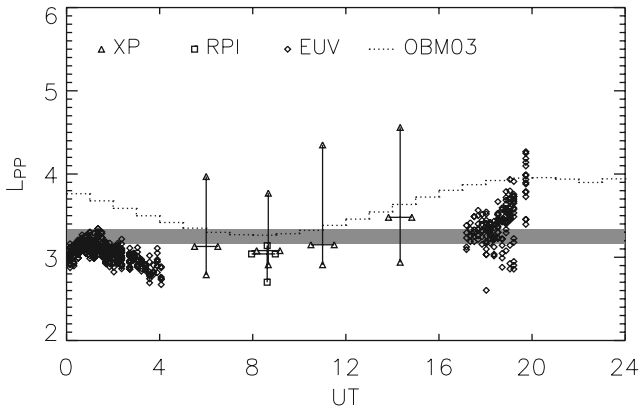

Figure 6. IMAGE EUV determined and [*O'Brien and Moldwin*, 2003] modeled plasmapause location as a function of UT throughout 14 May 2001, for the local meridian monitored by the ground-based magnetometers. Cross-phase and IMAGE RPI estimates of the location of the 1000, 500 and 100 amu/cm^3 densities are also shown. See text for details.

eigenfrequency may be inferred (see Figure 1). Such a scenario would also explain the apparent localized density increase along the 0600 UT profiles at $3.5 \lesssim L \lesssim 4.0$ (Figures 5b and 5e).

[23] The question arises as to why the negative cross-phase maximum was only observed for a few hours. One scenario involves flux tube filling, with a possible minor contribution from field line shortening or lengthening: Between 0600 UT and 0800 UT, refilling of smaller volume, partially filled plasmaspheric flux tubes, and larger volume depleted plasma trough flux tubes occurred. Because of the different flux tube volumes, the lower invariant latitude plasmaspheric flux tube density would increase faster than the higher invariant latitude plasma trough flux tubes, steepening the plasmapause gradient, creating a positive eigenfrequency gradient, and causing the cross-phase maximum polarity reversal from positive to negative. During this time interval the T01 model field lines were shortening by an increasing amount with increasing invariant latitude. This would act to increase the eigenfrequency with increasing UT, by an increasing amount with increasing invariant latitude, contributing to the first cross-phase maximum polarity reversal.

[24] The second cross-phase maximum polarity reversal, from negative to positive, which occurred at 1200–1230 UT, may be explained by continued plasma trough refilling decreasing the plasmapause density gradient with L shell, causing the removal of the positive eigenfrequency gradient through the plasmapause. Between 1100 UT and 1430 UT the T01 model predicts field line lengthening of all field lines modeled, by an increasing amount with increasing invariant latitude (possibly in response to the decreasing solar wind speed and IMF Bz strength). This would act to decrease the eigenfrequency by an increasing amount with increasing invariant latitude, contributing to the removal of the positive eigenfrequency gradient across the plasmapause.

[25] An entirely different scenario to explain the observed cross-phase maximum polarity reversals involves subcorotation of the plasmasphere [e.g., *Burch et al.*, 2004] such that the region monitored by the ESK-LER and GML-LER station pairs alternated from the plasmasphere to the plasmapause and back to the plasmasphere again, for example. However, in this scenario one would expect other, additional, station pairs to also observe a negative cross-phase maximum pre-0730 UT and post-1230 UT (the times at which the cross-phase maximum polarity reversals are observed in Figure 4); and the negative cross-phase maximum to occur at a significantly different frequency than the positive maximum as the higher density region was encountered. This was not the case.

[26] Figure 6 shows IMAGE EUV determined plasmapause locations as a function of UT through 14 May for the meridian monitored by the ground-based magnetometers (UT + 0h35 < MLT < UT + 3h01). Also plotted are the statistically expected plasmapause location determined via the [*O'Brien and Moldwin*, 2003] Dst based empirical model (OBM03); and dipole model derived cross phase and IMAGE RPI determined 1000, 500, and 100 amu/cm^3 locations, values which approximately demarcate the plasmapause in Figure 5. The upper (lower) point shows the 100 (1000) amu/cm^3 location, while the horizontal bars have been placed at the 500 amu/cm^3 location and show the UT interval which these values represent. The horizontal grey band highlights the L shell region where the cross-phase maximum polarity reversal was observed.

[27] The EUV data in Figure 5 show that prior to 0400 UT the plasmapause resided between L = 2.6 and L = 3.3, and after 1600 UT it resided between L = 2.6 and L = 4.3 (no data are available between these times, as the satellite passed through perigee). This indicates an outward moving plasmapause through the dayside sector, passing through the region where the cross-phase maximum polarity reversals were monitored. The cross-phase results, which assume a dipolar geomagnetic field, show the 500 amu/cm^3 location to be inward of L = 3.16 prior to 1430 UT, and outward of L = 3.34 at 1430 UT. This indicates a refilling, outward moving plasmapause region throughout 14 May 2001. The results of the OBM03 model also show a statistical expectation of an outward moving plasmapause through the dayside sector, being in close agreement with the cross-phase results.

[28] The question also arises as to why such negative cross-phase maxima are not observed more frequently. *Menk et al.* [2004] describe the expectation of a cross-phase maximum polarity reversal at the plasmapause and the difficulties in monitoring it. These include requiring a suitably wide, linear plasmapause; and spatial resolution issues of ground-based magnetometers located at eigenfrequency turning points. The RPI determined eigenfrequency profile in Figure 5 (calculated assuming a solely H^+ plasma, dipolar geomagnetic field geometry and r^{-1} radial density distribution along field lines) shows a steep positive gradient between L = 3.0 and L = 3.2, and a shallower positive gradient between L = 3.8 and L = 4.1. These indicate regions where the plasma mass density is expected to have a local gradient steeper than r^{-8}. According to the RPI profile the ESK station (L = 2.78) was at the foot of a field line in the plasmasphere, the GML station (L = 3.08) was at

the foot of a field line on the cusp of the plasmasphere and plasmapause, and the LER station (L = 3.63) was at the foot of a field line in the plasma trough. The cross-phase technique assumes that broadband energy excites all field lines at all frequencies, including their fundamental resonance frequency (eigenfrequency). However, because the resonance frequency of any particular field line will not usually dominate the amplitude spectra, this alone cannot be used to identify a field line eigenfrequency. Instead, the amplitude and phase difference spectra from two latitudinally separated magnetometer stations will allow determination of the eigenfrequency of the field line with a foot point at the midpoint of the two magnetometers. For this method to be successful, a coherence of at least 0.5, and preferably 0.7, should exist between the two spectra. If two the field lines of the two stations map to two different regimes inside and outside the plasmapause, then one might expect coherence to decrease. Also, if two individual field line eigenfrequencies are very different, one would not expect the cross-phase technique to be successful because the amplitude peak and 180° phase changes would occur at two distinct frequencies separated by more than their frequency width. Under such conditions, a measurable phase difference would not be distinguishable above that generated from phase differences associated with noise in the two spectra. Clearly neither of these potential issues caused the cross-phase technique to completely fail for this event, possibly because the density gradient at the plasmapause was only just steep enough to cause the positive eigenfrequency gradient (recall that it remained close to the density $\propto r^{-8}$ curve throughout the day).

[29] Straddling different regimes may or may not cause a negative cross-phase maximum, depending upon the gradient between the field line resonance frequencies of the two field lines being monitored above each of the ground magnetometers. This explains why not all station pairs straddling different regimes resulted in a negative cross-phase maximum.

4. Conclusion

[30] In this study we have presented observations of a dynamically varying cross-phase maximum polarity, monitored by ground-based magnetometer station pairs with midpoints at L = 3.16 and L = 3.34, through 14 May 2001. IMAGE RPI results show that a steep plasmapause resided in this region on this day. Cross-phase and T01 model results offer an explanation of the cross-phase maximum polarity reversals in terms of flux tube refilling, with a smaller contribution from field line morphology variations. IMAGE EUV results imply an outward moving plasmapause through the dayside sector, supporting this scenario.

[31] The plasma mass density gradient monitored across the plasmapause is close to the theoretical requirement for a negative cross-phase maximum to be observed (density variations steeper than r^{-8}). Previous work has demonstrated the ability of the cross-phase technique for monitoring plasmaspheric and plasma trough densities as well as plasmapause location, as a function of time. The results presented in this study highlight another important feature of the cross-phase technique, that is, monitoring dynamic plasmapause gradients and determining conditions associated with especially steep gradients, using only one pair of ground-based magnetometers.

[32] **Acknowledgments.** The IMAGE magnetometer data are collected as a Finnish-German-Norwegian-Polish-Russian-Swedish project, and we thank those institutes which maintain the array. The IMAGE magnetometer data were provided by the Finnish Meteorological Institute. BGS is a NERC funded facility, and SAMNET is a PPARC National Facility currently operated by Lancaster University. We thank the SAMNET team for providing the SAMNET and BGS magnetometer data. The authors thank B. W. Reinisch and B. R. Sandel for IMAGE RPI and EUV data, respectively. R. E. McGuire at SSC Web is acknowledged for the IMAGE satellite orbit data. Z. C. D. was funded by a PPARC studentship during part of this study. I. R. M. is supported by a Canadian NSERC discovery grant.

[33] Zuyin Pu thanks David Berube and another reviewer for their assistance in evaluating this paper.

References

Allan, W., F. W. Menk, B. J. Fraser, Y. Li, and S. P. White (1996), Are low-latitude pi2 pulsations cavity/waveguide modes?, *Geophys. Res. Lett.*, *23*, 765–768.

Baransky, L. N., S. P. Belokris, Y. E. Borovkov, and C. A. Green (1990), Two simple methods for the determination of the resonance frequencies of magnetic field lines, *Planet. Space Sci.*, *38*(12), 1573–1576.

Burch, J. L., J. Goldstein, and B. R. Sandel (2004), Cause of plasmasphere corotation lag, *Geophys. Res. Lett.*, *31*, L05802, doi:10.1029/2003GL019164.

Carpenter, D. L. (1978), Whistlers and VLF noises propagating just outside the plasmapause, *J. Geophys. Res.*, *83*(1), 45–57.

Carpenter, D. L., and R. R. Anderson (1992), An ISEE/whistler model of equatorial electron density in the magnetosphere, *J. Geophys. Res.*, *97*(A2), 1097–1108.

Carpenter, D. L., and R. L. Smith (1964), Whistler measurements of electron density in the magnetosphere, *Rev. Geophys.*, *2*(3), 415–441.

Dent, Z. C., I. R. Mann, F. W. Menk, J. Goldstein, C. R. Wilford, M. A. Clilverd, and L. G. Ozeke (2003), A coordinated ground-based and IMAGE satellite study of quiet-time plasmaspheric density profiles, *Geophys. Res. Lett.*, *30*(12), 1600, doi:10.1029/2003GL016946.

Dent, Z. C., I. R. Mann, J. Goldstein, F. W. Menk, and L. G. Ozeke (2006), Plasmaspheric depletion, refilling, and plasmapause dynamics: A coordinated ground-based and IMAGE satellite study, *J. Geophys. Res.*, *111*, A03205, doi:10.1029/2005JA011046.

Denton, R. E., et al. (2006), Realistic magnetospheric density model for 29 August 2000, *J. Atmos. Sol. Terr. Phys.*, *68*, 615–628.

Fraser, B. J., J. L. Horwitz, and J. A. Slavin (2002), Are ULF wave observations affected by the plasmapause in the presence of heavy ion mass loading of the geomagnetic field?, paper presented at Workshop on the Application of Radio Science, Natl. Comm. for Radio Sci., Sydney, Australia.

Fraser, B. J., J. L. Horwitz, J. A. Slavin, Z. C. Dent, and I. R. Mann (2005), Heavy ion mass loading of the geomagnetic field near the plasmapause and ULF wave implications, *Geophys. Res. Lett.*, *32*, L04102, doi:10.1029/2004GL021315.

Goldstein, J., M. Spasojevic', P. H. Reiff, B. R. Sandel, W. T. Forrester, D. L. Gallagher, and B. W. Reinisch (2003), Identifying the plasmapause in IMAGE EUV data using IMAGE RPI in situ steep density gradients, *J. Geophys. Res.*, *108*(A4), 1147, doi:10.1029/2002JA009475.

Goldstein, J., B. R. Sandel, M. F. Thomsen, M. Spasojevic', and P. H. Reiff (2004), Simultaneous remote sensing and in situ observations of plasmaspheric drainage plumes, *J. Geophys. Res.*, *109*, A03202, doi:10.1029/2003JA010281.

Gough, H., and D. Orr (1984), The effect of damping on geomagnetic pulsation amplitude and phase at ground observatories, *Planet. Space Sci.*, *32*(5), 619–628.

Green, J. L., S. Boardsen, S. F. Fung, H. Matsumoto, K. Hashimoto, R. R. Anderson, B. R. Sandel, and B. W. Reinisch (2004), Association of kilometric continuum radiation with plasmaspheric structures, *J. Geophys. Res.*, *109*, A03203, doi:10.1029/2003JA010093.

Lee, D.-H., and K. Kim (1999), Compressional MHD waves in the magnetosphere: A new approach, *J. Geophys. Res.*, *104*(A6), 12,379–12,385.

Lemaire, J. F., K. I. Gringauz, D. L. Carpenter, and V. Bassolo (1998), *The Earth's Plasmasphere*, Cambridge Univ. Press, Cambridge, U.K.

Loto'aniu, T. M., C. L. Waters, B. J. Fraser, and J. C. Samson (1999), Plasma mass density in the plasmatrough: Comparison using ULF waves and CRRES, *Geophys. Res. Lett.*, *26*(21), 3277–3280.

Lühr, H., A. Aylward, S. C. Buchert, A. Pajunpää, K. Pajunpää, T. Holmboe, and S. M. Zalewski (1998), Westward moving dynamic substorm features

observed with the Image magnetometer network and other ground-based instruments, *Ann. Geophys.*, *16*, 425–440.
Menk, F. W., D. Orr, M. A. Clilverd, A. J. Smith, C. L. Waters, D. K. Milling, and B. J. Fraser (1999), Monitoring spatial and temporal variations in the dayside plasmasphere using geomagnetic field line resonances, *J. Geophys. Res.*, *104*(A9), 19,955–19,969.
Menk, F. W., I. R. Mann, A. J. Smith, C. L. Waters, M. A. Clilverd, and D. K. Milling (2004), Monitoring the plasmapause using geomagnetic field line resonances, *J. Geophys. Res.*, *109*, A04216, doi:10.1029/2003JA010097.
Milling, D. K., I. R. Mann, and F. W. Menk (2001), Diagnosing the plasmapause with a network of closely spaced ground-based magnetometers, *Geophys. Res. Lett.*, *28*(1), 115–118.
O'Brien, T. P., and M. B. Moldwin (2003), Empirical plasmapause models from magnetic indices, *Geophys. Res. Lett.*, *30*(4), 1152, doi:10.1029/2002GL016007.
Orr, D., and H. W. Hanson (1981), Geomagnetic pulsation phase patterns over an extended latitudinal arrray, *J. Atmos. Terr. Phys.*, *43*(9), 889–910.
Poulter, E. M., W. Allan, J. G. Keys, and E. Nielsen (1984), Plasmatrough ion mass densities determined from ULF pulsation eigenperiods, *Planet. Space Sci.*, *32*(9), 1069–1078.
Reinisch, B. W., et al. (2000), The Radio Plasma Imager investigation on the Image spacecraft, *Space Sci. Rev.*, *91*, 319–359.
Sandel, B. R., et al. (2000), The extreme ultraviolet imager investigation for the Image mission, *Space Sci. Rev.*, *91*(1–2), 197–242.
Shiokawa, K., T. Ogawa, H. Oya, F. J. Rich, and K. Yumoto (2001), A stable auroral red arc observed over Japan after an interval of very weak solar wind, *J. Geophys. Res.*, *106*(A11), 26,091–26,102.
Thorne, R. M., and R. B. Horne (1992), The contribution of ion-cyclotron waves to electron heating and SAR-arc excitation near the storm-time plasmapause, *Geophys. Res. Lett.*, *19*, 417–420.
Tsyganenko, N. A. (2002a), A model of the near magnetosphere with a dawn-dusk asymmetry 1. Mathematical structure, *J. Geophys. Res.*, *107*(A8), 1179, doi:10.1029/2001JA000219.
Tsyganenko, N. A. (2002b), A model of the near magnetosphere with a dawn-dusk asymmetry 2. Parameterization and fitting to observations, *J. Geophys. Res.*, *107*(A8), 1176, doi:10.1029/2001JA000220.
Waters, C. L. (2000), ULF resonance structure in the magnetosphere, *Adv. Space Res.*, *25*(7/8), 1541–1558.
Waters, C. L., F. W. Menk, and B. J. Fraser (1991a), The resonance structure of low latitude Pc3 geomagnetic pulsations, *Geophys. Res. Lett.*, *18*(12), 2293–2296.
Waters, C. L., F. W. Menk, B. J. Fraser, and P. M. Ostwald (1991b), Phase structure of low-latitude Pc3–4 pulsations, *Planet. Space Sci.*, *39*(4), 569–582.
Waters, C. L., J. C. Samson, and E. F. Donovan (1996), Variation of plasmatrough density derived from magnetospheric field line resonances, *J. Geophys. Res.*, *101*(A11), 24,737–24,745.
Waters, C. L., K. Takahashi, D.-H. Lee, and B. J. Anderson (2002), Detection of ultralow-frequency cavity modes using spacecraft data, *J. Geophys. Res.*, *107*(A10), 1284, doi:10.1029/2001JA000224.
Yeoman, T. K., D. K. Milling, and D. Orr (1990), Pi2 pulsation polarization patterns on the U.K. sub-auroral magnetometer network (SAMNET), *Planet. Space Sci.*, *38*(5), 589–602.

Z. C. Kale, I. R. Mann, and L. G. Ozeke, Department of Physics, University of Alberta, Edmonton, AB, Canada, T6G 2G7. (zkale@phys.ualberta.ca; imann@phys.ualberta.ca; lozeke@phys.ualberta.ca)

J. Goldstein, Space Science and Engineering Division, Southwest Research Institute, 6220 Culebra Road, San Antonio, TX 78238, USA. (jgoldstein@swri.edu)

F. W. Menk and C. L. Waters, School of Mathematical and Physical Sciences, University of Newcastle, Callaghan, NSW 2308, Australia. (fred.menk@newcastle.edu.au; colin.waters@newcastle.edu.au)